



Published in final edited form as:

Neurol Lett. 2023 April ; 2(1): 16–24. doi:10.52547/nl.2.1.16.

Regional cerebral blood flow and brain atrophy in mild cognitive impairment and Alzheimer's disease

Fardin Nabizadeh^{1,2,*}, Mohammad Balabandian^{1,2}, Mohammad Reza Rostami^{1,2}, Soraya Mehrabi^{3,4}, Mohsen Sedighi^{4,5},
Alzheimer's Disease Neuroimaging Initiative**

¹Neuroscience Research Group (NRG), Universal Scientific Education and Research Network (USERN), Tehran, Iran.

²School of medicine, Iran University of Medical Sciences, Tehran, Iran

³Department of Physiology, Faculty of Medicine, Iran University of Medical Science, Tehran, Iran.

⁴Department of Neuroscience, Faculty of Advanced Technologies in Medicine, Iran University of Medical Science, Tehran, Iran.

⁵Neuroscience Research Center (NRC), Iran University of Medical Sciences, Tehran, Iran

Abstract

Objectives: A decline in the regional cerebral blood flow (CBF) is proposed to be one of the initial changes in the Alzheimer's disease process. To date, there are limited data on the correlation between CBF decline and gray matter atrophy in mild cognitive impairment (MCI) and AD patients. to investigate the association between CBF with the gray matter structural parameters such as cortical volume, surface area, and thickness in AD, MCI, and healthy controls (HC).

Methods: Data from three groups of participants including 39 HC, 82 MCI, and 28 AD subjects were obtained from the Alzheimer's disease Neuroimaging Initiative (ADNI). One-way ANOVA and linear regression were used to compare data and find a correlation between structural

**Data used to prepare this article were obtained from the Alzheimer's disease Neuroimaging Initiative (ADNI) database (adni.loni.usc.edu). As such, the investigators within the ADNI contributed to the design and implementation of ADNI and/or provided data but did not participate in the analysis or writing of this report. A complete listing of ADNI investigators can be found at: http://adni.loni.usc.edu/wp-content/uploads/how_to_apply/ADNI_Acknowledgement_List.pdf

*Corresponding Authors: Fardin Nabizadeh, ¹ Neuroscience Research Group (NRG), Universal Scientific Education and Research Network (USERN), Tehran, Iran; fardinnabizade1378@gmail.com.

Author contribution

FN and MB conceived and designed research. FN and MR analyzed data. FN, MB, MR, SM, and MS wrote the manuscript. All authors read and approved the manuscript.

Conflict of interest

The authors declare no conflict of interest regarding the publication of this paper.

Ethical approval

Since the data in this paper were obtained from the ADNI database (adni.loni.usc.edu), it does not include any research involving human or animal subjects.

Consent for publication

This manuscript has been approved for publication by all authors.

Consent to participate

Not applicable

parameters such as cortical volume, surface area, and thickness and CBF which measured by arterial spin labeling (ASL)-MRI.

Results: Our findings revealed a widespread significant correlation between the CBF and structural parameters in temporal, frontal, parietal, occipital, precentral gyrus, pericalcarine cortex, entorhinal cortex, supramarginal gyrus, fusiform, precuneus, and pallidum.

Conclusion: CBF decline may be a useful biomarker for MCI and AD and accurately reflect the structural changes related to AD. According to the present results, CBF decline, as measured by ASL-MRI, is correlated with lower measures of structural parameters in AD responsible regions. It means that CBF decline may reflect AD-associated atrophy across disease progression and is also used as an early biomarker for AD and MCI diagnosis.

Keywords

Alzheimer's Disease; cerebral blood flow; atrophy; mild cognitive impairment

1. Introduction

Alzheimer's disease (AD) is a type of neurodegenerative disease characterized by learning and memory impairment, personality changes, and executive dysfunction (1). Although mental status examination and neuropsychological tests have been applied to assess the symptoms of mild cognitive impairment (MCI) and AD patients, neuroimaging methods such as magnetic resonance imaging (MRI) are used to identify structural changes in the AD brain (2).

Neuroimaging findings revealed that multiple atrophy patterns are associated with MCI and AD (3, 4) which can help clinical guidelines to more accurately and earlier diagnose AD (5). Moreover, the rate of whole-brain atrophy is a valuable marker to predict the progression of AD in patients with MCI (6). Mainly, the patterns of atrophy were observed in the medial temporal lobe (7, 8), hippocampus, and posterior cingulate cortex of AD patients (9).

A decline in the regional cerebral blood flow (CBF) is proposed to be one of the initial changes in the AD process (10). Many investigations reported hypoperfusion in several brain regions such as the posterior cingulate gyrus and precuneus in MCI and AD patients (11, 12). However, the cause of this decline is not fully understood to date. Mattsson et al. reported an association between the Amyloid β deposition and CBF pattern and also demonstrated that declined CBF is an early consequence of neural death prior to considerable grey matter loss (13). CBF can be quantified by Arterial Spin Labeling Magnetic Resonance Imaging (ASL-MRI), a non-invasive technique with a short acquisition time utilized in many studies for detecting hypoperfusion patterns in MCI and AD patients (14).

To date, there are limited data on the correlation between CBF decline and gray matter atrophy in MCI and AD patients (15). Investigating the correlation between CBF and structural parameters of the brain might expand our knowledge on pathological pathways involved in the cortical and subcortical changes of the brain. Therefore, the present study was undertaken to investigate the association between CBF with the gray matter structural

parameters such as cortical volume, surface area, and thickness in regions known to be affected by AD progression in three groups of individuals, including healthy controls (HC), MCI, and AD subjects.

2. Materials and Methods

Participants and data acquisition

The participants' information was collected from the Alzheimer's Disease Neuroimaging Initiative (ADNI) database (<http://www.loni.usc.edu/>), launched by Michael W. Weiner in 2003, as a public-private partnership. The primary endpoint of ADNI has been to examine whether serial MRI, positron emission tomography (PET), biological marker examinations, and clinical/neuropsychological assessments can be combined to determine the progression of MCI and early AD. All participants with available data and imaging results were enrolled in this study. Demographic and clinical data of 149 subjects including 28 AD patients, 82 MCI patients, and 39 healthy subjects were obtained from the ADNI and analyzed in this study. The diagnostic status, Mini-Mental State Examination (MMSE) score, and the result of apolipoprotein E gene (APOE) genotyping for each subject were collected, as well. Regions of interests (ROIs) including left and the right hippocampus, ACC, insula, inferior parietal cortex, middle frontal cortex, inferior temporal cortex, pre-central cortex, post-central cortex, caudate-middle frontal cortex, and frontal poles, inferior frontal gyrus, superior frontal gyrus, inferior parietal gyrus, inferior temporal gyrus, middle temporal gyrus, post-central cortex, caudate-middle frontal cortex, entorhinal cortex, precuneus, and fusiform were entered to our analyses.

MRI acquisition (T1, FLAIR)

All ADNI individuals had T1 structural MRI and T2-FLAIR acquired on a 1.5 Tesla (T) or 3T scanner from Siemens, Philips, or General Electric. The ADNIMRI protocol is described in detail by Jack et al. (16). Accordingly, axial 3T FLAIR was acquired with voxel sizes of $0.85994 \times 0.8594 \times 5$ mm. Each image underwent quality control after acquisition at the Mayo Clinic (Rochester, MN), including image quality assessment, protocol compliance checks, and inspection for clinically significant medical abnormalities.

Automatic segmentation with Freesurfer V 4.3 and 5.1

Volumetric segmentation was performed using the FreeSurfer image analysis suite, which is freely available for download online (<http://surfer.nmr.mgh.harvard.edu/>). The processing consisted of motion correction of multiple T1-weighted images, removal of non-brain tissues, automated Talairach transformation, segmentation of subcortical white matter and gray matter structures, automated topology correction, and intensity normalization. For the quality control, the outcomes of the image were represented as Pass, Fail, Hippocampus-Only, and Partial. Only images with the overall outcome of pass remained.

Arterial spin labeling (ASL)-MRI processing

ASL-MRI, as a completely non-invasive procedure, was used to measure the CBF by exploiting the endogenous spins of arterial water as a proxy for blood flow. Also, labeling magnetization of arterial spins was inverted selectively. The Center for Imaging of

Neurodegenerative Diseases (CIND) prepared perfusion-weighted images (PWI), computed a map of CBF, and conducted a regional analysis with Freesurfer V 4.3. ASL-MRI pre-processing consisted of three steps. PWI computations were done and the ASL images were separated into the two groups of tagged and untagged after motion correction, and the mean of each group was computed and saved. Next, the difference in the mean of the two groups was determined to obtain the PWI. The first untagged image was used as the reference for water density and termed “M0”. M0 was used to calibrate the ASL signal for CBF computations and estimate the transformation from ASL-MRI and structural MRI, as an intermediate frame. The control (M0) image is scaled to estimate a map of the blood magnetization, M_{blood} by correcting for the lower density of tissue water relative to arterial blood water, λ , and for the different relaxation characteristics of tissue and arterial blood water, as follows:

$$M_{\text{blood}} = \frac{M0}{\lambda} e^{(R^*_{\text{tissue}} - R^*_{\text{blood}}) T E}$$

where λ is the blood/water ratio in tissue, R^* is the two relaxation rates and $T E$ is the blood relaxation time. The third step was intensity scaling of PWI, as well as the M0 image. After geometric distortion correction and partial volume correction, the CBF was quantified in physical units by normalizing ASL to an estimated blood water density signal

Statistical analysis

Before the statistical analysis, variables without a normal distribution were log-transformed to meet the normality assumption. Demographic variables were compared between the groups using the ANOVA and Kruskal–Wallis for parametric and non-parametric variables respectively. Local associations between the CBF and structural variables were investigated using multivariable linear regression models. Regression models were implemented for each association separately by adding CBF parameters and structural variables (i.e., cortical volume, thickness, and surface area) for each region as dependent and independent variables while entering age, sex, and APOE- ϵ 4 genotyping status as controlled variables. The bootstrapping method was used for addressing type I errors due to multiple comparisons (17, 18). The significance level was set at 0.05, and statistical analysis was performed in SPSS version 22.

3. Results

Participants' characteristics

Table 1 presents the demographic and clinical data of the participants. There was no significant difference in terms of age, education, and sex among the groups. However, AD patients had significantly lower MMSE scores and more APOE- ϵ 4 carriers as compared to the MCI and HC groups.

Local correlation between CBF and thickness

In all AD patients, negative correlations were found in two regions, including the posterior segment of the left middle frontal gyrus and the caudal part of the right anterior cingulate

cortex (Table 2). The results of Pearson's correlation analysis showed a positive correlation between the CBF and thickness in several regions in the MCI group, including left entorhinal area, left and right lateral occipital cortices, left and right superior parietal lobules, right inferior parietal lobule, posterior part of the right middle frontal gyrus, right superior frontal gyrus, right inferior temporal gyrus, right pericalcarine, right postcentral gyrus, right precentral gyrus. In contrast, we found a negative correlation between right anterior cingulate cortex thickness and CBF. In healthy subjects, significant correlations were found between the left entorhinal area and the rostral part of the left anterior cingulate cortex with CBF.

Local correlation between CBF and cortical volume

Pearson correlation coefficient revealed a significant correlation between the CBF and cortical volume in the MCI and HC groups but not in the AD group (Table 3). In the MCI group, significant positive correlations were observed between CBF and following regions: left and right postcentral gyrus, left and right precentral gyrus, left and right precuneus, right precuneus, left and right posterior cingulate cortex, caudal and rostral parts of the left anterior cingulate, right superior frontal gyrus, left and right superior parietal lobules, right inferior parietal lobule, left and right superior temporal gyri, right transverse temporal gyrus, left and right inferior temporal gyri, left middle temporal gyrus, left temporal gyrus, right lateral occipital gyrus, left and right supramarginal gyri, right insula, left entorhinal cortex, and right bankssts. In the HC group, significant positive correlations were found between CBF and left and right superior parietal gyri, right supramarginal gyrus, left entorhinal cortex, left fusiform gyrus, left medial orbital gyrus, anterior part of the left middle frontal gyrus, left temporal gyrus, right inferior temporal gyrus, and rostral part of the left anterior cingulate cortex.

Local correlation between CBF and surface area

Investigation of the local correlation between the CBF and surface area in the groups of the study revealed that this correlation in the AD patients was meaningful in the left inferior temporal gyrus and isthmus of the left cingulate gyrus, as shown in Table 4. In the MCI group, this significance was more than other groups and was found in the left and right precuneus, right superior and inferior parietal lobules, right superior temporal gyrus, left and right transverse temporal gyri, left inferior and middle temporal gyri, left temporal pole, caudal and rostral parts of the left anterior cingulate gyrus, left posterior cingulate gyrus, left supramarginal gyrus, right middle orbital gyrus, right bankssts, and right fusiform gyrus. Moreover, significant correlations in the HC group were attributed to the following regions: right precentral gyrus, left and right superior parietal lobules, left and right supramarginal gyri, left fusiform gyrus, left and right lateral occipital gyri, right inferior and middle temporal gyri, and the orbital part of the left inferior frontal gyrus.

Regions of interest are shown for a significant correlation between structural parameters and regional cerebral blood flow in Figure 1.

4. Discussion

In the present study, our findings showed a significant correlation between the CBF decline and gray matter atrophy in widespread regions measured as cortical volume, surface area, and thickness in HC, MCI, and AD subjects.

Recently, in contrast to our results, Kim et al. revealed no significant association between the CBF and cortical thickness in MCI patients and healthy people (19). In contrast to our findings, Luckhaus et al. found no significant association between atrophy and CBF in the early pathogenesis of AD (20). Generally, the CBF decline is one of the earliest events observed in patients with AD (21). Evidence on CBF changes in patients with MCI revealed that an increase or decrease in perfusion can be an early marker of neurodegeneration and may reflect metabolic demand changes in regions that are involved in cognitive function, including the temporal lobe, parietal lobe, frontal lobe, posterior cingulate gyrus, and precuneus (22, 23). The same patterns of atrophy especially in the medial temporal lobe also observed in AD and MCI patients (24, 25). There is a study that investigated the pattern of atrophy and CBF decline in AD and MCI patients reported both cerebral perfusion and gray matter structure reduced in the entorhinal cortex and the isthmus cingulate cortex (26).

Our findings revealed that changes in the CBF are associated with structural parameters in various regions of the gray matter in AD, MCI, and HC subjects. The correlations were mostly found in the medial temporal, parietal, occipital, frontal, cingulate, and precuneus, which are thought to be enrolled in the early pathology of AD and cognitive decline (27). In line with our findings, Soman et al., there was a positive correlation between CBF and gray matter volume of the temporal neocortex (15). However, we found correlations in more regions such as the frontal, parietal, occipital, precentral gyrus, pericalcarine cortex, entorhinal cortex, supramarginal gyrus, fusiform, and pallidum. Notably, we found a correlation between the CBF and cortical volume and surface area in the posterior cingulate cortex and temporal pole of MCI patients, which are the main regions in the default mode network (DMN) (28). It should be mentioned that this association was mostly observed in MCI patients.

According to our results, the CBF can reflect atrophy in the responsible regions in course of AD; however, the mechanisms of this hypoperfusion in the early stages of neurodegeneration are unclear. Evidence shows that the CBF decline can lead to A β and hyperphosphorylated tau accumulation (29). On the other hand, A β monomers have been found to drive vasoconstriction in brain arterioles and potentially contribute to a reduction in resting cerebral blood flow and, therefore, CBF decline could be the result of A β pathology (30). Recent studies suggest that A β can impair the fundamental mechanisms of blood supply regulation (31, 32). However, several factors might account for this dysregulation in AD, such as impairment of endothelium-dependent responses, the hypercontractile phenotype of cerebral smooth muscle cells, and vascular oxidative stress (33). In this regard, Michels et al. observed a significant relationship between the CBF and APOE- ϵ 4, independent of A β accumulation in MCI and normal elderly individuals (34).

Significant correlations between the CBF and structural changes in the main brain regions involved in AD development, including the cingulate gyrus, temporal gyrus, parietal lobule, precuneus, and middle frontal gyri have been found in our study (25, 34). There was a significant correlation between CBF and cortical volume and surface area in the precuneus which is not surprising considering its function in visuospatial perception, episodic memory retrieval, and consciousness. Moreover, patients with MCI had lower cortical thickness in the precuneus compared to normal people (35).

Our study has certain limitations such as a small sample size which influences the analyses. Also, our study is cross-sectional, so we are unable to examine the longitudinal association between CBF and structural parameters.

5. Conclusion

According to the present results, CBF decline, as measured by ASL-MRI, is correlated with lower measures of structural parameters in AD responsible regions. It means that CBF decline may reflect AD-associated atrophy across disease progression and is also used as an early biomarker for AD and MCI diagnosis. However, there are some unresolved issues regarding the exact underlying pathology of CBF decline in AD development; therefore, further research is needed in this area. CBF decline may be a useful biomarker for MCI and AD and accurately reflect the structural changes related to AD.

Acknowledgments

Data collection and sharing for this project was funded by the Alzheimer's Disease Neuroimaging Initiative (ADNI) (National Institutes of Health Grant U01 AG024904) and DOD ADNI (Department of Defense award number W81XWH-12-2-0012). ADNI is funded by the National Institute on Aging, the National Institute of Biomedical Imaging and Bioengineering, and through generous contributions from the following: AbbVie, Alzheimer's Association; Alzheimer's Drug Discovery Foundation; Araclon Biotech; BioClinica, Inc.; Biogen; Bristol-Myers Squibb Company; CereSpir, Inc.; Cogstate; Eisai Inc.; Elan Pharmaceuticals, Inc.; Eli Lilly and Company; EuroImmun; F. Hoffmann-La Roche Ltd and its affiliated company Genentech, Inc.; Fujirebio; GE Healthcare; IXICO Ltd.; Janssen Alzheimer Immunotherapy Research & Development, LLC.; Johnson & Johnson Pharmaceutical Research & Development LLC.; Lumosity; Lundbeck; Merck & Co., Inc.; Meso Scale Diagnostics, LLC.; NeuroRx Research; Neurotrack Technologies; Novartis Pharmaceuticals Corporation; Pfizer Inc.; Piramal Imaging; Servier; Takeda Pharmaceutical Company; and Transition Therapeutics. The Canadian Institutes of Health Research is providing funds to support ADNI clinical sites in Canada. Private sector contributions are facilitated by the Foundation for the National Institutes of Health (www.fnih.org). The grantee organization is the Northern California Institute for Research and Education, and the study is coordinated by the Alzheimer's Therapeutic Research Institute at the University of Southern California. ADNI data are disseminated by the Laboratory for Neuro Imaging at the University of Southern California.

Funding

We do not have any financial support for this study.

Availability of data and material

The datasets analyzed during the current study are available upon request with no restriction.

References

1. Sedighi M, Baluchnejadmojarad T, Fallah S, Moradi N, Afshin-Majdd S, Roghani M. Klotho Ameliorates Cellular Inflammation via Suppression of Cytokine Release and Upregulation of

- miR-29a in the PBMCs of Diagnosed Alzheimer's Disease Patients. *Journal of molecular neuroscience* : MN. 2019;69(1):157–65. [PubMed: 31197641]
2. Johnson KA, Fox NC, Sperling RA, Klunk WE. Brain imaging in Alzheimer disease. *Cold Spring Harbor perspectives in medicine*. 2012;2(4):a006213–a. [PubMed: 22474610]
 3. Vemuri P, Whitwell JL, Kantarci K, Josephs KA, Parisi JE, Shiung MS, et al. Antemortem MRI based STructural Abnormality iNdex (STAND)-scores correlate with postmortem Braak neurofibrillary tangle stage. *NeuroImage*. 2008;42(2):559–67. [PubMed: 18572417]
 4. Pini L, Pievani M, Bocchetta M, Altomare D, Bosco P, Cavado E, et al. Brain atrophy in Alzheimer's Disease and aging. *Ageing Research Reviews*. 2016;30:25–48. [PubMed: 26827786]
 5. Dubois B, Feldman HH, Jacova C, Cummings JL, Dekosky ST, Barberger-Gateau P, et al. Revising the definition of Alzheimer's disease: a new lexicon. 2010. p. 1118–27.
 6. Whitwell JL. Progression of Atrophy in Alzheimer ' s Disease and Related Disorders. 2010:339–46.
 7. Berron D, van Westen D, Ossenkoppele R, Strandberg O, Hansson O. Medial temporal lobe connectivity and its associations with cognition in early Alzheimer's disease. *Brain*. 2020;143(3):1233–48. [PubMed: 32252068]
 8. Stranahan AM, Mattson MP. Selective vulnerability of neurons in layer II of the entorhinal cortex during aging and Alzheimer's disease. *Neural Plasticity*. 2010;2010.
 9. Scheff SW, Price DA, Ansari MA, Roberts KN, Schmitt FA, Ikonovic MD, et al. Synaptic change in the posterior cingulate gyrus in the progression of Alzheimer's disease. *Journal of Alzheimer's Disease*. 2015;43(3):1073–90.
 10. Korte N, Nortley R, Attwell D. Cerebral blood flow decrease as an early pathological mechanism in Alzheimer's disease. *Acta Neuropathologica*. 2020;140(6):793–810. [PubMed: 32865691]
 11. Dai W, Lopez OL, Carmichael OT, Becker JT, Kuller LH, Gach HM. Mild cognitive impairment and alzheimer disease: patterns of altered cerebral blood flow at MR imaging. *Radiology*. 2009;250(3):856–66. [PubMed: 19164119]
 12. Binnewijzend MA, Kuijer JP, Benedictus MR, van der Flier WM, Wink AM, Wattjes MP, et al. Cerebral blood flow measured with 3D pseudocontinuous arterial spin-labeling MR imaging in Alzheimer disease and mild cognitive impairment: a marker for disease severity. *Radiology*. 2013;267(1):221–30. [PubMed: 23238159]
 13. Mattsson N, Tosun D, Insel PS, Simonson A, Jack CR, Beckett LA, et al. Association of brain amyloid- β with cerebral perfusion and structure in Alzheimer's disease and mild cognitive impairment. *Brain*. 2014;137(5):1550–61. [PubMed: 24625697]
 14. Kaneta T, Katsuse O, Hirano T, Ogawa M, Shihikura-Hino A, Yoshida K, et al. Voxel-wise correlations between cognition and cerebral blood flow using arterial spin-labeled perfusion MRI in patients with Alzheimer's disease: a cross-sectional study. *BMC Neurol*. 2017;17(1):91. [PubMed: 28506213]
 15. Soman S, Raghavan S, Rajesh PG, Varma RP, Mohanan N, Ramachandran SS, et al. Relationship between Cerebral Perfusion on Arterial Spin Labeling (ASL) MRI with Brain Volumetry and Cognitive Performance in Mild Cognitive Impairment and Dementia due to Alzheimer's Disease. *Ann Indian Acad Neurol*. 2021;24(4):559–65. [PubMed: 34728951]
 16. Jack CR Jr, Slomkowski M, Gracon S, Hoover TM, Felmlee JP, Stewart K, et al. MRI as a biomarker of disease progression in a therapeutic trial of milameline for AD. *Neurology*. 2003;60(2):253–60. [PubMed: 12552040]
 17. Parra-Frutos I Controlling the Type I error rate by using the nonparametric bootstrap when comparing means. *The British journal of mathematical and statistical psychology*. 2013;67.
 18. Wang F-K, Yang S Applying Bootstrap method to the types I–II errors in the measurement system. *Quality and Reliability Engineering International*. 2008;24:83–97.
 19. Kim CM, Alvarado RL, Stephens K, Wey HY, Wang DJJ, Leritz EC, et al. Associations between cerebral blood flow and structural and functional brain imaging measures in individuals with neuropsychologically defined mild cognitive impairment. *Neurobiology of aging*. 2020;86:64–74. [PubMed: 31813626]
 20. Luckhaus C, Cohnen M, Flüss MO, Jänner M, Grass-Kapanke B, Teipel SJ, et al. The relation of regional cerebral perfusion and atrophy in mild cognitive impairment (MCI) and early Alzheimer's dementia. *Psychiatry research*. 2010;183(1):44–51. [PubMed: 20541374]

21. Shirayama Y, Takahashi M, Oda Y, Yoshino K, Sato K, Okubo T, et al. rCBF and cognitive impairment changes assessed by SPECT and ADAS-cog in late-onset Alzheimer's disease after 18 months of treatment with the cholinesterase inhibitors donepezil or galantamine. *Brain imaging and behavior*. 2019;13(1):75–86. [PubMed: 29247294]
22. Wierenga CE, Dev SI, Shin DD, Clark LR, Bangen KJ, Jak AJ, et al. Effect of mild cognitive impairment and APOE genotype on resting cerebral blood flow and its association with cognition. *Journal of cerebral blood flow and metabolism : official journal of the International Society of Cerebral Blood Flow and Metabolism*. 2012;32(8):1589–99. [PubMed: 22549621]
23. Wolk DA, Detre JA. Arterial spin labeling MRI: an emerging biomarker for Alzheimer's disease and other neurodegenerative conditions. *Current opinion in neurology*. 2012;25(4):421–8. [PubMed: 22610458]
24. Pettigrew C, Soldan A, Zhu Y, Wang M-C, Moghekar A, Brown T, et al. Cortical thickness in relation to clinical symptom onset in preclinical AD. *Neuroimage Clin*. 2016;12:116–22. [PubMed: 27408796]
25. Parker TD, Slattery CF, Zhang J, Nicholas JM, Paterson RW, Foulkes AJM, et al. Cortical microstructure in young onset Alzheimer's disease using neurite orientation dispersion and density imaging. *Human brain mapping*. 2018;39(7):3005–17. [PubMed: 29575324]
26. Wirth M, Pichet Binette A, Brunecker P, Köbe T, Witte AV, Flöel A. Divergent regional patterns of cerebral hypoperfusion and gray matter atrophy in mild cognitive impairment patients. *Journal of cerebral blood flow and metabolism : official journal of the International Society of Cerebral Blood Flow and Metabolism*. 2017;37(3):814–24. [PubMed: 27037094]
27. Buckner RL, Andrews-Hanna JR, Schacter DL. The brain's default network: anatomy, function, and relevance to disease. *Annals of the New York Academy of Sciences*. 2008;1124:1–38. [PubMed: 18400922]
28. Moskowitz MA, Lo EH, Iadecola C. The science of stroke: mechanisms in search of treatments. *Neuron*. 2010;67(2):181–98. [PubMed: 20670828]
29. Niwa K, Younkin L, Ebeling C, Turner SK, Westaway D, Younkin S, et al. Abeta 1–40-related reduction in functional hyperemia in mouse neocortex during somatosensory activation. *Proceedings of the National Academy of Sciences of the United States of America*. 2000;97(17):9735–40. [PubMed: 10944232]
30. Niwa K, Kazama K, Younkin L, Younkin SG, Carlson GA, Iadecola C. Cerebrovascular autoregulation is profoundly impaired in mice overexpressing amyloid precursor protein. *American journal of physiology Heart and circulatory physiology*. 2002;283(1):H315–23. [PubMed: 12063304]
31. Chow N, Bell RD, Deane R, Streb JW, Chen J, Brooks A, et al. Serum response factor and myocardin mediate arterial hypercontractility and cerebral blood flow dysregulation in Alzheimer's phenotype. *Proceedings of the National Academy of Sciences of the United States of America*. 2007;104(3):823–8. [PubMed: 17215356]
32. Michels L, Warnock G, Buck A, Macaudo G, Leh SE, Kaelin AM, et al. Arterial spin labeling imaging reveals widespread and A β -independent reductions in cerebral blood flow in elderly apolipoprotein epsilon-4 carriers. *Journal of cerebral blood flow and metabolism : official journal of the International Society of Cerebral Blood Flow and Metabolism*. 2016;36(3):581–95. [PubMed: 26661143]
33. Kim SM, Kim MJ, Rhee HY, Ryu CW, Kim EJ, Petersen ET, et al. Regional cerebral perfusion in patients with Alzheimer's disease and mild cognitive impairment: effect of APOE epsilon4 allele. *Neuroradiology*. 2013;55(1):25–34. [PubMed: 22828738]
34. Cheng CP, Cheng ST, Tam CW, Chan WC, Chu WC, Lam LC. Relationship between Cortical Thickness and Neuropsychological Performance in Normal Older Adults and Those with Mild Cognitive Impairment. *Aging and disease*. 2018;9(6):1020–30. [PubMed: 30574415]
35. Csukly G, Sirály E, Fodor Z, Horváth A, Salacz P, Hidasi Z, et al. The Differentiation of Amnesic Type MCI from the Non-Amnesic Types by Structural MRI. *Front Aging Neurosci*. 2016;8:52. [PubMed: 27065855]

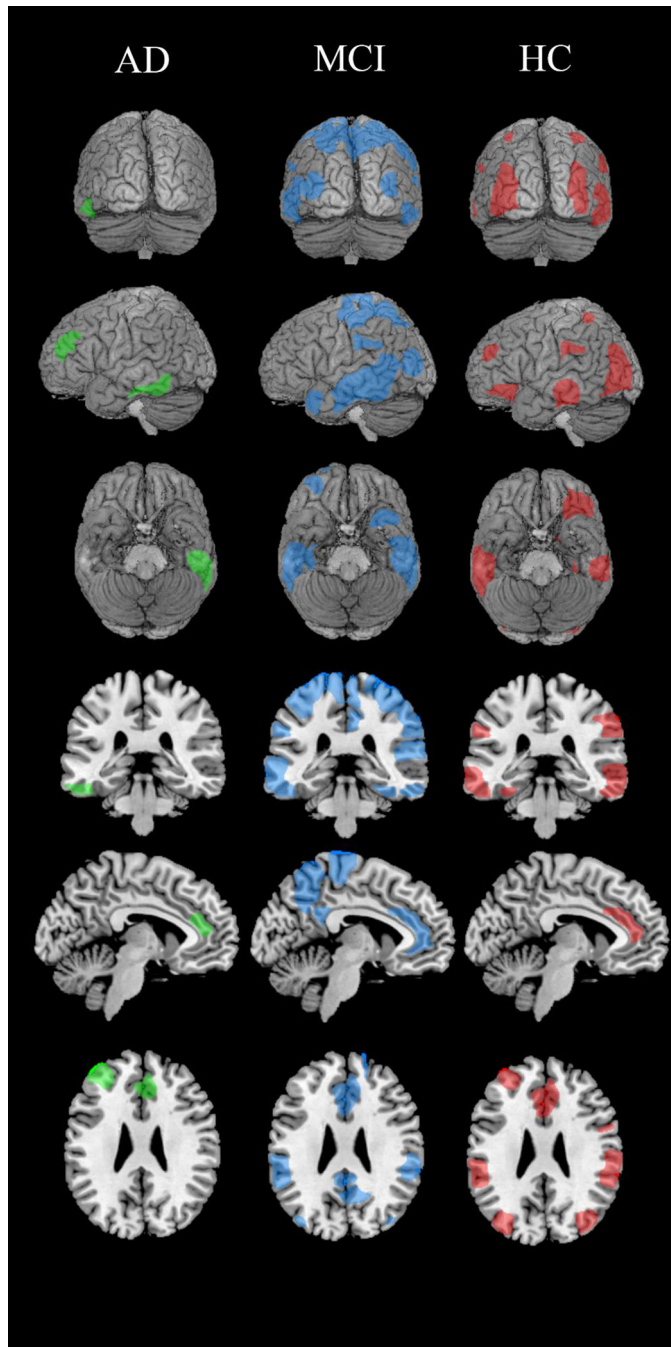


Figure. Regions of interest are shown for significant correlation between structural parameters and regional cerebral blood flow. AD (green), MCI (blue), HC (red). Alzheimer's Disease (AD), mild cognitive impairment (MCI), healthy controls (HC).

Table1.

Participants characteristic

Variables	HC(39)	MCI(82)	AD(28)	P value
Age, years	71.8(±6.8)	70.4(±7.4)	73.1 (±6.5)	0.186
Gender(M/F)	15/24	41/41	14/14	0.469
Education, years	16.2(±2.5)	16.5(2.7)	16.5(±2.2)	0.829
MMSE	28.9(±1.4)	28.3(±1.6)	23.9(±1.9)	0.000
APOE genotype				0.000
With out ε4	26	53	8	
One ε4	11	22	12	
Two ε4	1	7	8	

HC: healthy controls, MCI: mild cognitive impairment, AD: Alzheimer's Disease, MMSE: mini mental state examination. Values are showed as mean ± SD. Results of One-way ANOVA analysis between groups noted as P value.

Table2.

Significant Results of partial correlation analyses of CBF and Thickness within groups

Regions	β coefficient	P value
AD		
Posterior part of left middle frontal	-0.457	0.033
Caudal part of right anterior cingulate	-0.544	0.005
MCI		
Left entorhinal area	0.237	0.035
Left lateral occipital	0.259	0.022
Right lateral occipital	0.284	0.012
Left superior parietal lobule	0.250	0.026
Right superior parietal	0.357	0.001
Posterior part of right middle frontal	0.288	0.010
Right inferior parietal	0.316	0.005
Right inferior temporal	0.299	0.011
Right pericalcarine	0.234	0.039
Right postcentral	0.231	0.040
Right precentral	0.307	0.006
Rostral part of right anterior cingulate	-0.243	0.031
Right superior frontal	0.303	0.007
HC		
Left entorhinal area	0.400	0.017
Rostral part of left anterior cingulate	0.523	0.001

Cerebral blood flow (CBF), Alzheimer's disease (AD), mild cognitive impairment (MCI), healthy controls (HC)

Table3.

Significant Results of partial correlation analyses of CBF and Cortical volume within groups

Regions	β coefficient	P value
MCI		
Right postcentral	0.284	0.011
Right posterior cingulate	0.234	0.038
Right precentral	0.286	0.011
Right precuneus	0.387	0.000
Right superior frontal	0.248	0.027
Right superior parietal	0.372	0.001
Right superior temporal	0.257	0.029
Right supramarginal	0.266	0.018
Right transverse temporal	0.244	0.030
Right insula	0.255	0.023
Caudal part of left anterior cingulate	0.272	0.015
Left entorhinal	0.301	0.007
Left inferior temporal	0.244	0.039
left middle temporal	0.302	0.010
Left paracentral	0.264	0.019
Left postcentral	0.268	0.017
Left posterior cingulate	0.256	0.023
Left precentral	0.288	0.010
Left precuneus	0.360	0.001
Rostral part of left anterior cingulate	0.372	0.001
Left superior parietal	0.297	0.008
Left superior temporal	0.268	0.023
Left supramarginal	0.320	0.004
Left temporal	0.296	0.012
right bankssts	0.258	0.022
Right inferior parietal	0.460	0.000
Right inferior temporal	0.351	0.003
Right lateral occipital	0.274	0.015
HC		
Right superior parietal	0.348	0.041
Right supramarginal	0.346	0.042
Left entorhinal	0.383	0.023
Left fusiform	0.401	0.021
Left medial orbital	0.385	0.022
Anterior part of left middle frontal	0.374	0.027
Left superior parietal	0.412	0.014
Left temporal	0.368	0.035
Right inferior temporal	0.406	0.019

Regions	β coefficient	P value
Rostral part of left anterior cingulate	0.523	0.001

Cerebral blood flow (CBF), Alzheimer's disease (AD), mild cognitive impairment (MCI), healthy controls (HC)

Author Manuscript

Author Manuscript

Author Manuscript

Author Manuscript

Table4.

Significant Results of partial Correlation Analyses of CBF and Surface area within groups

Regions	β coefficient	P value
AD		
Left inferior temporal	0.441	0.031
Isthmus of left cingulate	0.458	0.021
MCI		
Right precuneus	0.315	0.005
Right superior parietal	0.254	0.024
Right superior temporal	0.279	0.018
Right transverse temporal	0.243	0.031
Caudal part of left anterior cingulate	0.367	0.001
Left inferior temporal	0.238	0.044
left middle temporal	0.283	0.016
Left posterior cingulate	0.249	0.027
Left precuneus	0.312	0.005
Rostral part of left anterior cingulate	0.387	0.000
Left supramarginal	0.297	0.008
Left temporal pole	0.259	0.028
Left transverse temporal	0.252	0.025
Right bankssts	0.282	0.012
Right fusiform	0.274	0.020
Right inferior parietal	0.338	0.002
Right middle orbital	0.269	0.017
HC		
Right precentral	0.379	0.025
Right superior parietal	0.411	0.014
Right supramarginal	0.383	0.023
Left fusiform	0.458	0.007
Left lateral occipital	0.388	0.021
Orbital part of left inferior frontal	0.385	0.022
Left superior parietal	0.441	0.008
Left supramarginal	0.388	0.021
Right inferior temporal	0.415	0.016
Right lateral occipital	0.498	0.002
Right middle temporal	0.456	0.008

Cerebral blood flow (CBF), Alzheimer's disease (AD), mild cognitive impairment (MCI), healthy controls (HC)